Radiative Closure Experiments at a Cloud-Free Desert Site, Nevada, as Part of MISR Algorithm Validation

J.E. Conel, W. A. Abdou, C J. Bruegge, B.J. Gaitley, M.C. Helmlinger, W. C. Ledeboer, S.H. Pilorz, and J.V. Martonchik
MISR Project
Jet Propulsion Laboratory
California Institute of Technology
Pasadena, CA91 109

ABSTRACT

Radiative closure experiments involving a comparison between surface-measured spectral irradiance anti the surface irradiance calculated according to a radiative transfer code at a desert site in Nevada under clear skies, yield the result that agreement between the two requires presence of an absorbing aerosol component with an imaginary refractive index equal to 0.03 and a 50:50 mix by optical depth of small and large particles with log-normal size distributions. The mode radius of the small particle distribution is 0.03 μm and that of the large 0.5 μm. The same aerosol model can be used for both day-to-day fits in one campaign year, and also between campaigns in different years. The high imaginary index required for the fits suggests presence of urban-type particles in the aerosol, but an alternative under study is to rely on absorbing iron oxide components in a dust fraction to account for some of the absorption.

INTRODUCTION

As part of the algorithm validation phase of preflight activities for the Multiangle Imaging SpectroRadiometer (MISR) and in conjunction with development of a so-called vicarious method of on-orbit absolute instrument radiometric calibration, a series of radiative closure experiments have been carried out under cloud-free conditions at a dry lake site (Lunar Lake) in central Nevada.

Vicarious calibration methods are entirely independent of the pre-launch laboratory and post-launch onboard methods, except for tracing of field instrument calibrations and calibration panels to NIST standards, and are consequently expected to play an important role in determination and maintenance of the MISR radiometric calibration over time. Vicarious calibration of satellite instruments involves the use of homogeneous naturally occurring ground targets that are large enough to encompass a number of satellite pixels. Dry lakes at moderate altitude in remote places of the southwestern United States have often been used for this purpose (see for example [l]), to minimize atmospheric scattering and absorption and water vapor interference. Cloud-free stable atmospheric conditions are also sought. The top-of-atmosphere (TOA) radiance at the sensor is calculated with a radiative transfer code (RTC) utilizing measured target reflectance over the area of several pixels together with atmospheric spectral optical depth, single scattering phase function and water vapor absorption. The TOA radiance so-obtained is assigned to the digital numbers measured by the satellite to obtain a reevaluation of the radiometric calibration coefficients for the sensor. Up to and including the present time, never in the field do direct observations of the composition or size distribution of the atmospheric aerosol burden accompany the other field measure-

ments, so that the aerosol compositional and size distribution model are left to be inferred from the indirect atmospheric radiation measurements.

In this report we have made use of closure results to improve the vicarious technique. Closure in the present instance implies agreement between the spectral irradiance measured at the surface by a diffuse/direct radiometer and the spectral irradiance calculated at the surface according to a standard radiative transfer code adopted by MISR. Such closure experiments provide a retrieval of aerosol properties, in the absence of direct measurements, specifically by forcing the calculated bottom-of-atmosphere (BOA) spectral irradiance to agree with observations. Although measured optical depths are typically incorporated into the vicarious RTC computations, the retrieval of aerosol refractive index and radius information, for vicarious applications, is newly described here.

MISR EXPERIMENT OVERVIEW

MISR is scheduled for launch on the EOS AM-1 platform in June, 1998. MISR will provide radiometrically calibrated, stable camera radiance measurements coregistered at nine view angles ($\pm 70.5°, \pm 60.0°, \pm 45.6°, \pm 26.1°, 0.0°$) and four wavelengths (446, 556,672, and 866 nm) globally over a 360 km swath of the Earth's surface on each pass. The fundamental cross-track pixel size at the surface is 275 m for the off-nadir pixels and 250 m in the nadir camera. From these 36 multiangle and multispectral observations, estimates of atmospheric aerosol abundance and composition, surface bidirectional reflectance properties, cloud top heights and albedo of surface and cloud layers will be obtained. Such observations will be employed among other things for improved determinations of the global aerosol burden, estimation of aerosol microphysical properties, identification of sources and sinks of aerosols, and for improved determination of surface and atmospheric radiation balance.

A principal MISR aerosol science data product is the column aerosol optical depth reported at a wavelength of 555 nm, together with aerosol type at a spatial sampling of 17.6 km globally. These retrievals are carried out by minimizing residuals between the observed multiangle and multispectral radiances on orbit and a pre-calculated radiance data set utilizing dry end-members and mixtures of globally representative aerosol types as functions of relative humidity together with prespecified surface reflectance types. These procedures are explained in detail in [2].

FIELD OBSERVATIONS, CALIBRATION, AND DATA REDUCTION METHODS

Field Site

Lunar Lake is a dry playa absolutely free of vegetation cover located in south central Nevada (Latitude 38 °24'N; Longitude 116°00'W) roughly 250 km NNW of Las Vegas. The bright uniform playa surface is oval in shape, about 5 km in long dimension (oriented NE) and 2 km across. The surface is at an elevation of approximately 1740 m. The surface is checked by a regular polygonal series of desiccation cracks that contribute small scale shadowing (I cm) for sun incidence angles other than at zenith. The site is relatively remote from major population centers and at moderate altitude, and was chosen in expectation of low aerosol turbidity. low atmospheric water vapor, and relatively long periods of cloud free conditions. Geologically the Lunar Lake playa resides in a partially fault bounded depression surrounded by a terrain consisting mainly of darker basaltic

flows and basaltic cinder deposits.

INSTRUMENTATION AND METHODS

Surface Reflectance. We estimated the hemispherical directional spectral reflectance (HDRF), at a nadir-view angle, of the playa surface from measurements taken with an Analytical Spectral Devices (ASD) portable spectrometer. The spectrometer covers the spectral range 350-2700 nm with a spectral sampling interval of 2 nm and spectral resolution of about 10 nm. Target measurements carried out at specific times of the day during approximately 1/2 hour to 1 hour measurement periods over grids of 48-60 points laid out on the surface in rectangular arrays covering pixel or multiple pixel size test areas. These surface measurements were interspersed with frequent measurements of a SpectraIon reference panel to help compensate for atmospheric effects, motion of the Sun, and stability of the radiometer. The grid array measurements were subsequently combined to obtain an average value for the test areas, and it is these values that are used to specify the reflectance boundary condition in the RTC for the modeling experiments. Under more turbid atmospheric conditions than encountered, the surface reflectance for downwelling radiation calculations might need to include contributions from the surrounding darker basaltic surface deposits, but this option has not been pursued here.

Atmospheric Measurements. Calibration Methods and Data Reduction. We made radiation measurements at the surface of both the direct solar beam and the global irradiance with two instruments: (1) Reagan sunphotometer, and (2) Yankee Environmental Systems (YES) Multifilter Rotating Shadowband Radiometer (MFRSR). The Reagan Sunphotometer, made by J.A. Reagan, University of Arizona, is a 10-channel automatically recording and sun-tracking instrument covering the channels 380, 400, 440, 520, 610, 670, 780, 870, 940, and 1030 nm with full-width half maximum (FWHM) widths between 7-17 nm. The MFRSR [3] provides automated recording and separation of total downwelling, direct-normal, and diffuse irradiances from six narrowband filter channels (each 10 nm) that are located at 415, 500, 610, 665, 862, and 935 nm together with one broadband unfiltered channel covering about 300-1000 nm. Both the Reagan and MFRSR data are used to provide estimates of aerosol spectral optical depth, ozone, and water vapor column abundances, and the MFRSR direct measurement of the surface downwelling spectral irradiance for comparison with RTC-calculated quantities. The residual optical depth for both instruments is provided by subtracting the Rayleigh component determined from a measurement of atmospheric pressure, in each case using a formula given by Hansen and Travis [4]. The aerosol and ozone optical depth components are retrieved from the residual optical depth simultaneously using an algorithm due to Flittner *et al.* [5], which requires no special assumption about the size distribution law (e.g., Junge) for its implementation apart from the condition that the retrieved aerosol optical depth variation with wavelength obey a minimum second-derivative constraint. We rely throughout on local field calibration of these radiometers, using the Langley method and aggregate intercept values obtained for all good observing days from fits in the morning hours confined between 5.5 to 1.8 airmasses. Errors on optical depths and irradiance measurements reflect uncertainty in the instrument calibration constants derived from this method for local conditions. For optical depths these errors range from 0.6-1.090.

Radiative transfer code. The monochromatic, one-dimensional RTC used in this study is based on the discrete ordinate matrix operator method of Grant and Hunt [6]. The associated

atmosphere/surface model is described by the number of atmospheric layers, the optical properties (aerosol and Rayleigh scattering optical depths, phase functions, and single scattering albedos) of each layer, the surface directional reflectance characteristics (analytical/empirical models or measurements), and the altitude of aircraft/spacecraft observations. In its current configuration the code computes the direct and diffuse components of the radiance fields and associated fluxes (irradiance and radiant exitance) at both the surface and the aircraft/spacecraft altitude. These results allow a direct comparison to measurements from the various ground-based instruments, from the MISR aircraft simulator AirMISR, or the imaging spectrometer AVIRIS, and also can be used as input to ancillary retrieval algorithms such as those used to derive full bidirectional reflectance factors for the surface. The code has been verified against a second code based on the Hansen-Travis [4] adding-doubling method. The results obtained by the two codes agree to within 0.1%.

FIELD OBSERVATIONS

We report here our closure studies from one of two annual EOS Intercomparison Campaigns (IC's), carried out May31 -June 7, 1996, at Lunar Lake. The results are compared in a preliminary way with those of a second campaign, June 23-27, 1997 also at Lunar Lake. Both of these IC's, which represented joint international activities among five EOS instrument groups, will be described elsewhere [7]. During these intensive observation periods by the MISR group, both Reagan and MFRSR observations were collected on a day-long basis. The data sets presented here represent data from the best observing times (e.g., no cirrus or other cloud cover) culled from the complete validation data sets taken directly by the MISR validation team.

RESULTS

Constraints and Initial Assumptions

The code simulations described herein are constrained by the field-measured spectral optical depths and the surface reflectance. The latter has been assumed for the present work to be Lambertian and estimated as the hemispherical-directional reflectance as measured in the field at the nadir-view angle. Full descriptions of the total BRF compared to Lambertian will be forthcoming.

For specification of the multilayer values required by the RTC, the atmosphere has been assumed . uniform in composition vertically and laterally.

Because direct aerosol compositional and size measurements were not available from this site for either IC, an aerosol model was initially chosen representing approximately a sulfate aerosol composition (K. Theme, personal communication) that had an assumed complex index $\mathbf{m}_{init}$ ($\mathbf{m}$ = n - iK) equal to 1.44- i 0.005, and a power law size distribution. A Junge parameter of 4.6 was calculated from the aerosol spectral optical depth data for one of the best observing days. However, when we assume the particle size distribution to follow a power law, the optical properties of the aerosol were very sensitive to the maximum and minimum sizes used. It is unrealistic to expect particle number density to increase without bound for smaller particles. Subsequently we continued the analysis using the log-normal size distribution with particle size and composition known to exist in the Earth's atmosphere. For example, these include the small and large size particles with mode radii of 0.03 and 0.5 μm as described by Shettle and Fenn [8] and the medium size par-

title with mode radius 0.07 μm, which represents the accumulation mode of sulfate and soot with mode radius 0.012 pm. The latter two particles are described by d'Almeida *et al.* [9]. We considered pure aerosol particles as well as mixtures consisting of two or more particle types mixed externally as described in [2] and [8]. We assumed the particles to be homogeneous and spherical in shape and used the Mie theory to calculate single scattering al bedos and phase functions. Irradiance at the surface was calculated using the RTC described above.

Model Calculations and Fits

Data used in the present analysis, including diffuse and direct irradiances, the aerosol optical depths and the surface spectral reflectance, were collected on June 2, 3, and 4 at 14:30.16:00, and 18:00 UCT, and are presented in Figure (1). The diffuse and direct irradiances are normalized to the exoatmospheric solar spectral irradiance, which is taken proportional to the instrument calibration constant (V_o) obtained by the Langley regression method as the instrument response at zero airmass. Using the initial aerosol model with complex refractive index $\mathbf{m}_{init}$ and log-normal distribution with mode radius 0.07 μm gave calculated sky irradiances -20% to 30% greater than the observations. In an attempt to resolve this discrepancy we studied the sensitivity of the calculated irradiances to the aerosol size distribution and complex index of refraction.

Examples of the results for variation of the real refractive index n (keeping the imaginary index constant at 0.0 or 0.005 corresponding to the initial model) are shown in Figures (2a) and (2b) for the large and small particles size distributions respectively. Comparing Figures (2a) and (2b) shows the calculated sky irradiance is more sensitive to changes in refractive index of the smaller particle size distribution, but only when the particles are absorbing, and more so at longer wavelengths.

Figures (2c) and (2d) show the effect of changing the imaginary index κ from 0.0 to 0.03 while keeping the refractive index n constant at a value of 1.44. The results in these two figures show large changes in the calculated sky irradiance with increasing particle absorption. The sensitivity is again much higher for the smaller particles. This is because particles are more effective scatterers of radiation at wavelengths comparable to or smaller than their sizes. Therefore by increasing the absorption of the smaller particles the sky irradiance at wavelengths larger than the particle size is strongly attenuated.

From Figure (2) , the larger particles, even with significant absorption index of 0.03, do not bring agreement between model calculation and observation, especially at shorter wavelengths. On the other hand increasing the absorption of the smaller particles may bring agreement with the measurements at the shorter wavelengths but will drastically attenuate the irradiances calculated at larger wavelengths.

A more realistic model would be a multimodal size distribution with complex compositional characteristics. Such a mixture however must be constrained by the measured optical depth, *i.e.,* must satisfy the relation $\tau_{aer} = k_{ext} NZ$ where k_{ext} is an effective extinction cross section per particle, N is the effective particle number density per unit volume, and Z the height of the aerosol column in the atmosphere. More specifically k_{ext} should have the same spectral shape as τ_{aer}. Several combinations of the above particle types were examined for agreement with the observations as

well as satisfying the above relation. Figure (3a) compares the aerosol optical depth and the effective extinction cross section for one of the mixtures, and Figure (3b) shows the sky irradiance simulated with this mixture compared to the MFRSR observations. This mixture consists of about 50% (by optical depth at 500 nm) of small particles and 50% of large particles. Both particle types have m = 1.44- i 0.03. At larger wavelengths (800 rim), the contribution to the aerosol optical depth of the larger particles increases to - 60%. The mixture has a single scattering albedo of - 0.7 at 500 nm, decreasing to 0.64 near 800 nm. If we assume the particles are contained in the tropospheric layer only, i.e., -5 km or more, then the effective particle number density would be on the order of 2×10^4 cm^{-3} or about 10^{10} particles cm^{-2}. This mixture can be generated from particles known to exist in the, Earth's atmosphere, such as a mixture of mostly small rural particles (40% by optical depth at 500 rim), 20% large rural particles (with mode radius of 0.5 pm), and 30% small urban. All three particle types are described in Shettle and Fenn [8]. The effective single scattering albedo of such a mixture is -0.70 at 500 nm, and the effective absorption index, 0.03. The effective number density is -6 x 10^4 cm^{-3}. Figure (3c) shows all the MFRSR data in comparison to RTC calculations using this aerosol mixture.

Interestingly, the composite aerosol model just described for the 1996 IC results can also be applied successfully to the 1997 IC MFRSR surface irradiance data. Thus for the Lunar Lake site, not only can the same aerosol model apply from day to day, but seemingly also from year to year.

Discussion

At issue is how to account for the large imaginary index required by the fits. The most prominent highly absorbing aerosol species commonly present in the atmosphere is described as soot, which is mostly of anthropomorphic origin. Soot is very widespread in continental regions and is a component of the average continental aerosol model of d'Almeida, *et al.* [9]. The presence of soot has been reported in rural and remote areas at large distances from urban areas where it is known to be abundantly present. For example, Mazurek, *et al.* [10] have analyzed visibility-reducing organic aerosols in the vicinity of Grand Canyon, some 350 km southeast of the present site, and determined up to 1% elemental carbon of uncertain, but not local origin, in their analyses. For comparisons of aerosol refractive indices, Ball and Robinson [1 1] determined an imaginary aerosol refractive index of about 0.05 for haze aerosols in the Central United States.

Another possibility for the absorbing component that is applicable especially in arid regions is iron oxide, either hydrated as goethite/limonite or unhydrated as hematite. Direct evidence for the presence of Fe^{+3} absorption and its general nature is seen in the spectral reflectance of the Lunar Lake playa itself (Figure 1a). The rapid decrease in reflectance at wavelengths short of about 800 nm, represents the long wavelength wing of a charge transfer band centered in the ultraviolet due to Fe^{+3}. Iron oxidation of this type is ubiquitous in arid regions of the southwest. For the aerosol components, dust particles can be expected to have discontinuous coatings or to be permeated with iron oxidation products, or perhaps the iron oxides may exist suspended independently. To illustrate (he potential strength of an iron oxide effect we quote data on the refractive index of hematite, $\mathbf{m}_{He}(\alpha\text{-}Fe_2O_3)$ given by Kerker, *et al.* [12]. For example, at 440 nm $\mathbf{m}_{He}$ = 2.22 - i 0.51 and at 550 nm $\mathbf{m}_{He}$ = 2.3- i 0.16. This possibility is under study

Kato, et al. [13] using high quality measurements and radiative transfer calculations, have sug-

gested the presence of an unaccounted-for absorbing gas to account for discrepancies such as those reported here between calculated and measured surface irradiances at the ARM site, Oklahoma.

All these possible explanations of the discrepancies between observation and RT calculations should be considered in future field measurements.

ACKNOWLEDGMENTS

We thank Phil Slater and Kurt Theme of the Optical Sciences Center, University of Arizona, for helpful discussions and much cooperation and help in the planning and execution of the field protram. This research was sponsored by the National Aeronautics and Space Administration under Contract to the Jet Propulsion Laboratory, California Institute of Technology.

REFERENCES

1. Slater, P. N., Biggar, S. F., Helm, R. G., Jackson, R.D. Mao, Y., Moran, S., Palmer, J., and Yuan, B., Reflectance-and radiance-based methods for the inflight absolute calibration of multispectral sensors; Remote Sens. Environ.; 198722, 11-37.

2. Diner, D. J., Abdou, W. A., Ackerman, T. P., Crean, K., Gordon, H. R., Kahn, R. A., Martonchik, J. V., Paradise, S. R., Pinty, B, Verstraete, M. M., Wang, M, and West, R. A., *Level* 2 *Aerosol Retrieval Algorithm Theoretical Basis,* JPL D- 11400, Rev. B; Jet Propulsion Laboratory, Pasadena, CA, 1996,8 lpp.

3. Harrison, L., Michalsky, J., and Berndt, J., Automated multifilter rotating shadowband radiometer: an instrument for optical depth and radiation measurements, Appl. Opt. 1994 33 22,5118-5125.

4. Hansen, J. E., and Travis, L. D., Light scattering in planetary atmospheres, Space Sci. Rev. 1974 16, 527-610.

5. Flittner, D. E., Herman, B. M., Theme, K. J., and Simpson, J. M., Total ozone and aerosol optical depths inferred from radiometric measurements in the Chappuis absorption band, J. Atmos. Sci. 1993 50 8, 1113-1121.

6. Grant, I. P., and Hunt, G. E., Solution of radiative transfer problems using the invariant S_n method, Mon. Not. R. astr. Sot. 1968 141, 27-41.

7. Theme, K., Schiller, S.,Conel, J., Arai, and Tsuchida. Results of the 1996, joint, EOS vicarious calibration campaign to Lunar Lake, Nevada. Metrologia, NEWRAD97 special issue.

8. Shettle, E. P., and Fenn, R. W.; *Models for the aerosol of the lower atmosphere and the effects of humidity variations on their optical properties,* AFGL-TR-79-0214, Air Force Geophysical Laboratory, Hanscomb AFB, MA, 1979, 94 pp.

9. d'Almeida, G. A., Koepke, P., and Shettle, E. P., *Atmospheric aerosols: Global climatology and radiative characteristics;* A. Deepak Publishing: Hampton, Virginia, 1991; pp 45-97.

10. Mazurek, M., Masonjones, M. C., Masonjones, H. D., Salmon, L.G., Cass, G. R., Hallock, K. A., and Leach, M., Visibility-reducing organic aerosols in the vicinity of Grand Canyon National Park: Properties observed by high resolution gas chromatography, J. Geophys. Res. **1997** 102 (D3), **3779-3793.**

11. Ball, R. J., and Robinson G. D., The origin of haze in the Central United States and its effect on solar irradiation, J. Appl. Meteor. 1982 21 171-188

12. Kerker, M, Scheiner, P., Cooke, D.D., and Kratohvil, J. P., Absorption index and color of colloidal hematite, Journal of Colloid and Interface Science 1979 71(1) 176-187.

13. Kato,S., Ackerman, T. P., Clothiauz, E.E., Mater, J. H., Mace, G.G., Weseley, M. L., Murcray, F., and Michalsky, J. Uncertainties in modeled and measured clear-sky surface shortwave irradiances, (Submitted to J. Geophys. Res. [revised April, 1997]).

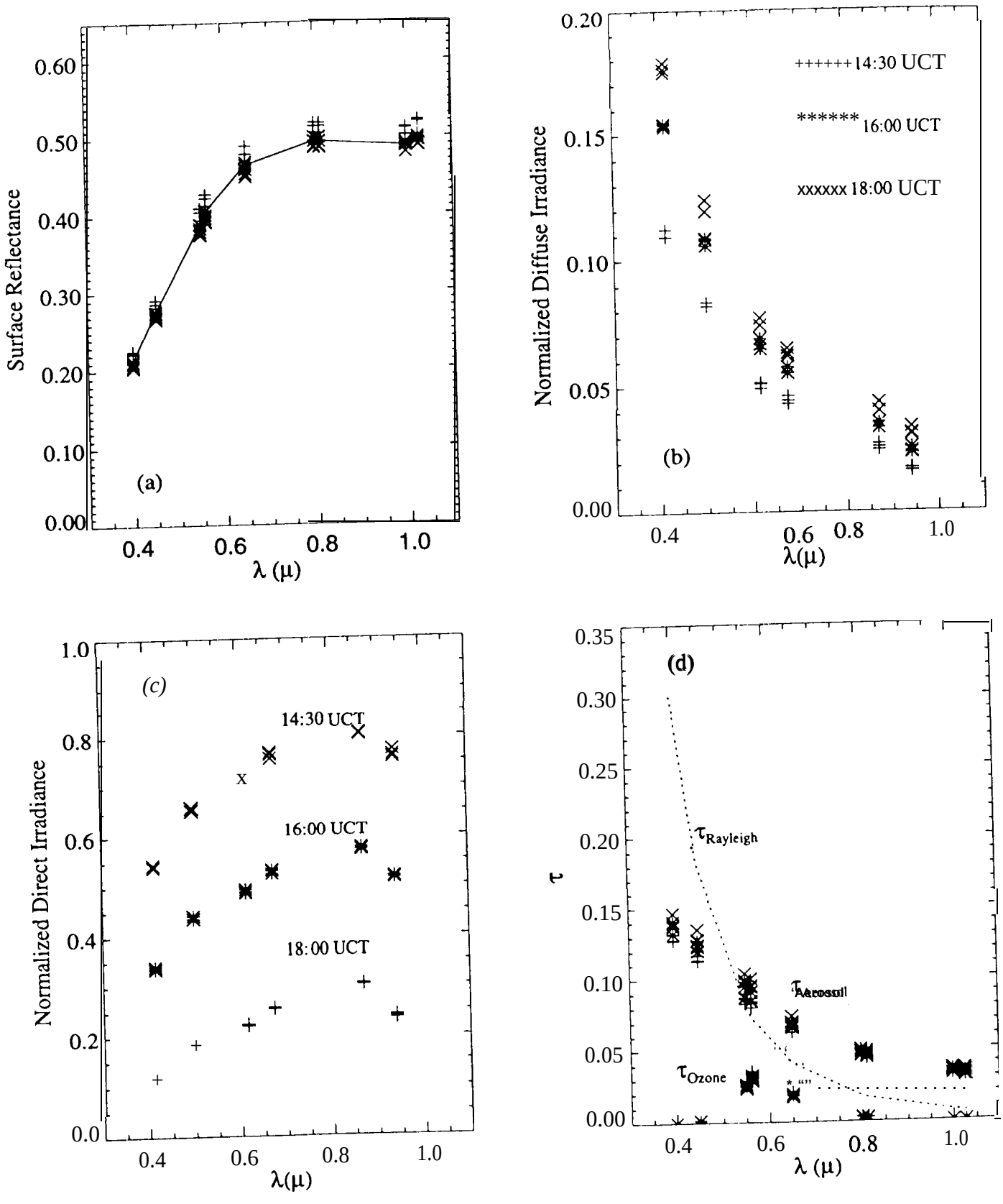

Figure 1. (a) Surface Reflectance (ASD), solid line is 10 nm resolution spectrum, (b) and (c) normalized diffuse and direct irradiance (MFRSR) and (d) optical depth retrieved from the sunphotometer.

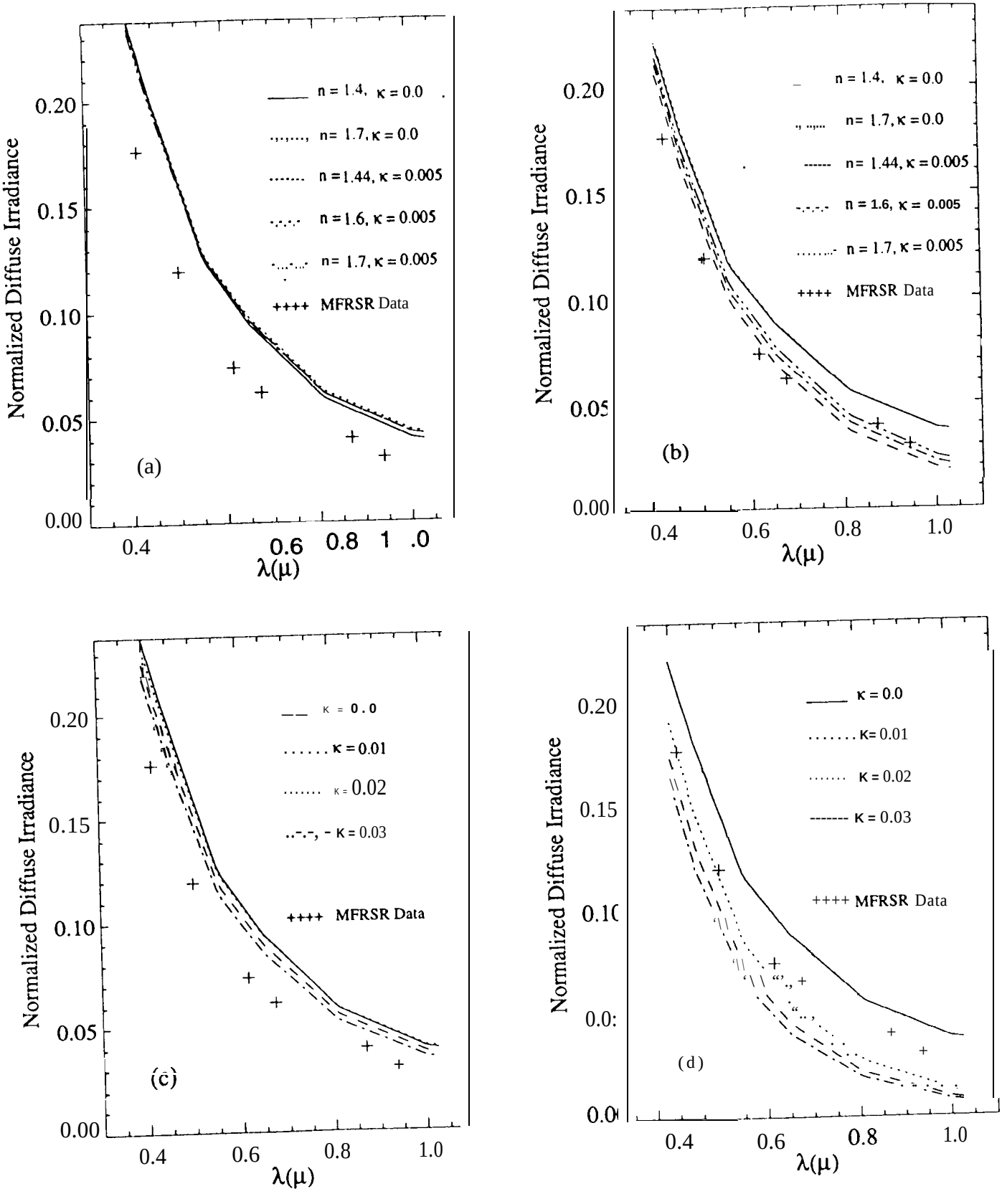

Figure 2. Sensitivity of calculated surface diffuse irradiance to change in refractive and absorption indecies. (a) and (c) for particles of $r_{mod} = 0.07\ \mu$ and (b) and (d) for the smaller particles of $r_{mod} = 0.03\ \mu$.

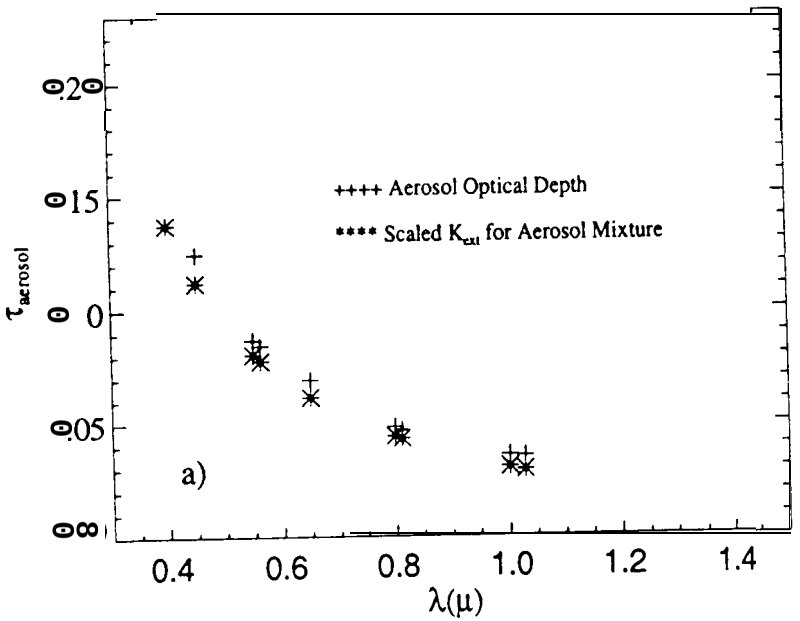

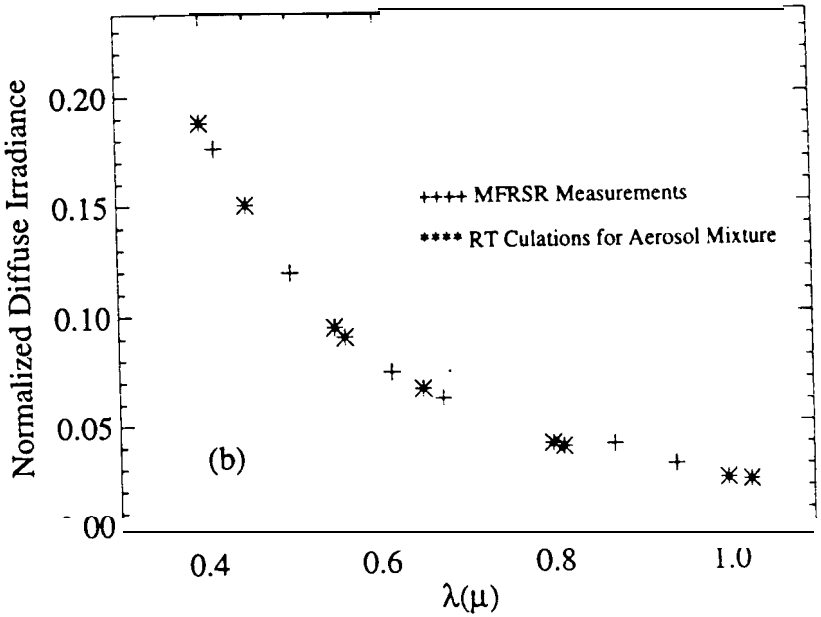

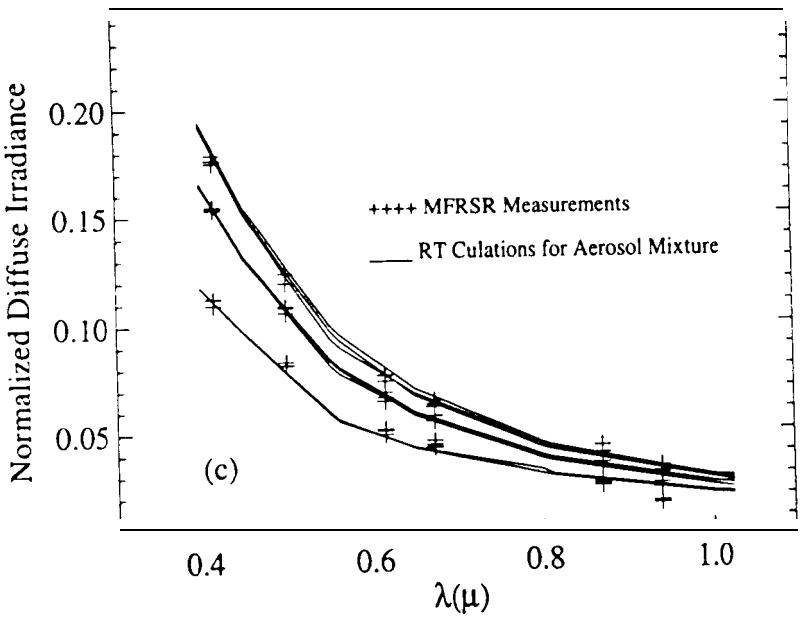

Figure 3. (a) The scaled variation of k_{ext} for a 50:50 mix, by optical depth, of small (r_{mod} = 0.03 μm) and large (r_{mod} = 0.5 μm) particles. (b) Comparison of the MFRSR measurements with the RT calculations for the above aerosol mixture. (c) comparison of the RT calculations for a mix of: 40% (by optical depth at 500 nm) , small rural, 30% large rural and 30% small urban aerosols with the MFRSR data on June 2 - 4 at 14:30, 16:00 and 18:00 UTC.